BEAM PROFILE MEASUREMENTS AND MATCHING AT SNS: PRACTICAL CONSIDERATIONS AND ACCOMMODATIONS*

Christopher K. Allen#, John D. Galambos, and Willem Blokland
ORNL, Oak Ridge, Tennessee 37831 USA

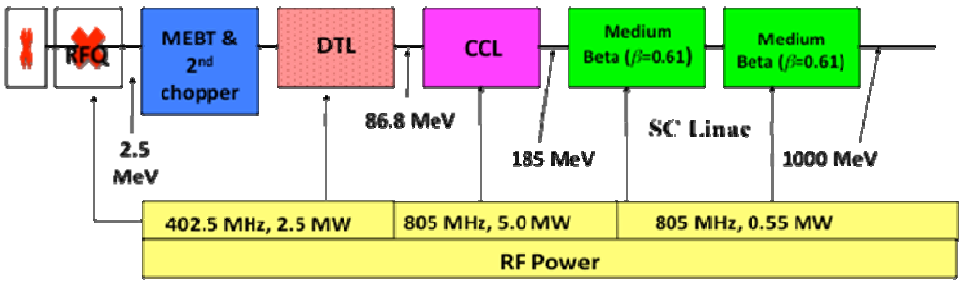

Figure 1: Schematic of SNS linac.

Abstract

Several issues are related to beam matching at SNS. Most concern the acquisition and processing of beam profile data, from which all the physics quantities are computed. There is a cascade of computational interdependence between these quantities, of concern is noise and measurement error which then propagate throughout. We present a quantitative investigation these errors, along with some matching results.

INTRODUCTION

The SNS linac is the world's highest power and highest energy H^- beam linear accelerator. Present operation is routinely at 1 MW, with a 925 MeV beam energy, 825 μs pulse length, 38 mA peak (23 mA average) current, and 60 Hz repetition rate. The front end section includes the ion source, an electrostatic Low Energy Beam Transport (LEBT) section that provides initial chopping, an RFQ (2.5 MeV exit energy) and a Medium Energy Beam Transport (MEBT) section which provides final stage chopping, transverse matching, and beam diagnostics. The primary accelerating structures are an 87MeV Drift Tube Linac (DTL), a 185 MeV Coupled Cavity Linac (CCL), and an elliptical-cell SuperConducting Linac (SCL) with final energy 925 MeV. The DTL is 37 m long with a radial aperture of 12.5 mm, the CCL section is 55 m long with a bore radius of 15 mm, and the superconducting section is 157 m long with a bore radius limitation of 35 mm (in the warm sections between the cryo-modules). Figure 1 shows a schematic of the linac architecture with the associated RF klystron main parameters.

Beam Loss is a major consideration along the linac, with a 1 W/m maximum for hands on maintenance. (This corresponds to residual activation below 100 mRem/hr at 30 cm several hours after shutdown.) An important factor in controlling losses is obtaining a well-matched transverse beam. To do so, and to understand halo growth along the linac, profile measurement stations are installed along the linac. Five wire profile monitors are installed in the MEBT yielding information about beam quality and matching into the DTL. There are 6 wire profile monitors in the DTL and 9 in the CCL. There are 9 laser profile measurement stations in the superconducting linac. In addition, there are 9 wire profile monitors in the High Energy Beam Transport (HEBT) section connecting the linac to the storage ring (not shown in Figure 2).

Table 1: Position and Size Calculations from Profile Data

	X Plane		Y Plane	
Quantity	μ	σ	μ	σ
Gauss fit	206.3507	1.9887	41.3546	5.4533
Statistical	206.344	5.0358	43.0695	12.7304
Stat. 1% NG	206.448	2.4891	44.0703	17.3715
Stat. 10% NG	206.42	2.0859	42.4341	5.07785

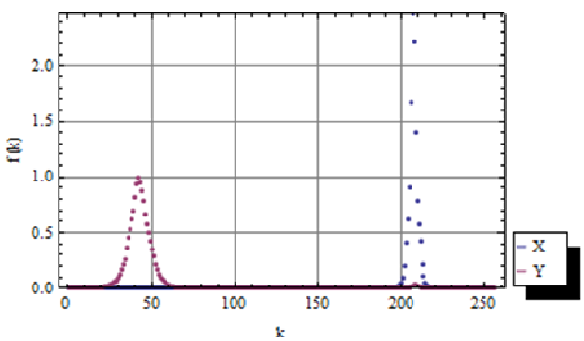

Figure 2: Profile data at SNS HEBT entrance.

BEAM SIZE CALCULATION

For any transverse matching algorithm, beam sizes along the matching section must be determined. The beam sizes are calculated from profile data obtained at the measurement stations [1]. The most common techniques are 1) direct statistical calculation, and 2) fitting the beam profile with a Gaussian distribution. The former technique

* This work supported by SNS through UT-Battelle, LLC, under contract DE-AC05-00OR22725 for the U.S. DOE.
#Corresponding author allenck@ornl.gov

is more general, as the beam distributions are not always Gaussian. However it is not easy to implement, results are noise sensitive. For the latter case, Gaussian fitting routines are robust but of questionable accuracy for beams with substantial halo. To illustrate we provide examples.

Figure 2 is a plot of profile data taken at the first wire scanner station of the SNS HEBT. Shown are data for both the horizontal X and vertical Y planes. The profiles are plotted against the scan actuator index k; there are 252 equally spaced steps. Table 1 contains the beam positions μ and sizes σ produced by the two different methods. All quantities are in units of actuator step length (to convert to distance multiply by step length). Also shown in Table 1 are statistical calculations after noise gating at 1% and 10% maximum level. This set provides an example of the volatility in the computations, especially for the beam size σ. Since the beam position are used to compute beam size, any noise or errors are propagated and amplified.

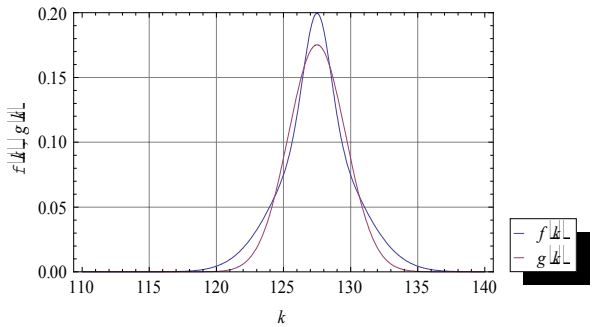

Figure 3: Non-Gaussian profile f and its Gaussian fit g.

Table 2: Non-Gaussian Profile Parameters

	Parameter			
	Ω	A	μ	σ
Exact	0	0.199471	127.5	2.64575
Gauss fit	2.78e-4	0.175117	127.5	2.11640
Statistical	0	0.18638	127.5	2.64575

With the direct statistical calculations one must know the noise mean (i.e., "floor") and variance. The mean is subtracted from all profile values while the variance is used to compute confidence intervals for the beam size. For more details see references [2] and [3].

Figure 3 shows a simulated situation where the direct calculation provides more accurate results. The blue curve f is a double-Gaussian profile with amplitude $A = 1/\sqrt{8\pi}$, position $\mu = 255/2$, and RMS size $\sigma = \sqrt{7}$; it is formed as the sum of two co-local, equal-magnitude Gaussian functions with standard deviations σ of 1 and 3. Profile f was sampled at axis locations $k = 1,2,\ldots,255$ to create the data set. (Figure 3 displays only $k = 110,\ldots,140$.) The red curve g is the Gaussian fit to this data set, found by least-square minimization. Table 2 lists the parameters of the Gaussian fit, along with the exact values in numerical form, and the statistical parameters computed directly. Parameter Ω in Table 2 is the noise mean. The high accuracy of the direct calculations follows from the absence of noise. However, the example illustrates how Gaussian fitting looses accuracy in the presence of halo.

Table 3: Profile Sampling vs. Information Content

σ	1	2	3	4	5
Info.	38%	68%	87%	95%	98.6%

Wire Scanner Step Size

The beam parameters are expressed in number of samples specifically to raise an issue concerning beam size and sampled data. It follows from the relationship between a signal and its Fourier transform, analogous to the uncertainty principle of quantum mechanics.

Say the distance between sample points is h. The Nyquist theorem states that the highest frequency component captured is $1/2h$. That is, we need to sample at twice the maximum signal frequency, otherwise information is lost. Assume our beam is Gaussian with standard deviation σh, σ being the number of samples per standard deviation. The Fourier transform is again a Gaussian, but with standard deviation $1/\sigma h$. To preserve all information the Fourier transform must be contained in the interval [-1/2h,+1/2h]. We cannot preserve all information, but we can use this fact to estimate the lost information content. The formula $1 - \mathrm{erf}\,\sigma/\sqrt{8}$ estimates the proportion of information retained using σ samples per standard deviation, producing Table 3. Then referring to Table 1 and Table 2 we see that only 70% to 80% of the profile information is retained.

Table 4: Horizontal Plane Beam Position and Size

	Chopper Off		Chopper On	
Station	μ	σ	μ	σ
WS104	-97.013	1.006	-96.846	1.139
WS106	-96.999	1.612	-97.041	1.591
WS110	-93.359	1.289	-93.428	1.316
WS204	-94.201	1.43	-94.106	1.466
WS210	-97.861	1.553	-97.979	1.597

Chopping Effects

Another concern at SNS is the effect of the beam chopper on measured beam size and, consequently, the resulting effect on Courant-Snyder parameter estimation and matching. Both choppers, in the MEBT and the LEBT, operate by steering the beam into plates at the up, down, left, and right positions. This action tends to produces a small periodic jitter in the positions of four consecutive mini-pulses. Table 4 lists the beam position μ and size σ measured at wire scanner locations along the CCL. From the table we can see that the chopper does have an effect, although it is probably insignificant.

COURANT-SNYDER PARAMETERS

Estimating the Courant-Snyder parameters for the beam is done using three or more beam size measurements in

conjunction with a beam propagation model (e.g., an envelope model). A beamline location is chosen (upstream of the measurements) and the Courant-Snyder parameters there are found numerically by minimizing the RMS error between the measurements and the model.

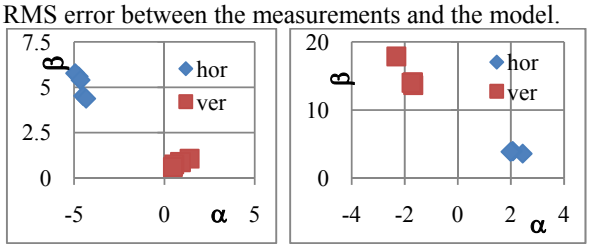

a) at CCL entrance b) at HEBT entrance

Figure 4: Courant-Snyder estimates.

To test the accuracy for estimated Courant-Snyder parameters we performed an experiment using four wire scanners placed between consecutive quadrupole magnets. The Courant-Snyder parameters were computed at an upstream location of all quadrupoles and wire scanners. The strength of each quadrupole was lowered by 5% and the Courant-Snyder parameters re-computed. Theoretically all results should be equal; however, due to measurement error, errors in the beam size calculation, and errors in the model, the values have variation.

Figure 4 are plots of the (α,β) Courant-Snyder parameters computed from the wire scanner measurements as described above. Figure 4a shows the estimates at the CCL entrance and Fig. 4b the HEBT entrance. The HEBT data has one outlier while the CCL data has more variation. This is likely due in part to the greater role of space charge at lower energy. Table 5 lists the mean values and their variances.

Table 5: Variance of Courant-Snyder Parameters

	α_x	β_x	α_y	β_y
CCL	-4.63±0.23	5.13±0.64	0.84±0.37	0.84±0.17
HEBT	2.14±0.21	3.83±0.17	-1.86±0.31	14.9±2.0

MATCHING

Matching is the proper shaping of the beam through a transition region. This is accomplished by setting the appropriate field strengths for matching quadrupole magnets. At SNS our best matching results have been for the HEBT. Even so, our current high-power production tune is not a matched beam condition. The reason for the irregularity is believed to be the presence of a small transverse halo; however, the physics of this situation is still being investigated. Our matching technique involves using a model in conjunction with a nonlinear search engine to predict the matching quadrupole strengths yielding desired Courant-Snyder parameters at a chosen match location. An alternate technique is to find magnet strengths that equalize beam sizes at periodic locations in a FODO lattice [4].

Figure 5 shows the results of one match iteration performed at the HEBT entrance. All figures show model-estimated beam envelopes derived from beam size measurements at four wire scanner locations. These measurements are highlighted in Fig. 5a) and 5c); Figure 5b) highlights the desired beam size at the match location. Figure 5a) shows the initial beam envelope through the match region. Figure 5b) is the model-predicted envelopes for the suggested quadrupole magnet settings provided by the matching algorithm. Figure 5c) is the actual beam envelope once these settings are sent to the machine. The beam is not in the predicted state; however, it is better conditioned than the initial state. Typically one must iterate this procedure several times to find a suitable match.

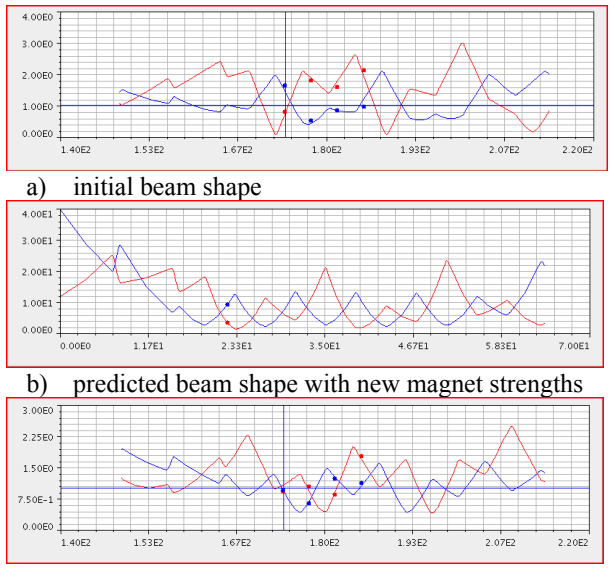

a) initial beam shape

b) predicted beam shape with new magnet strengths

c) actual beam shape with new magnet strengths

Figure 5: Matching results at the HEBT entrance.

SUMMARY

Several independent steps are needed in the matching process: profile measurements, beam size calculation, Courant-Snyder parameter estimation, and calculation of matching quadrupole strengths. At each stage errors are introduce which then propagate through the calculations. We have attempted to systematically study these errors in order to implement better matching strategies.

REFERENCES

[1] M. Plum, W. Christensen, R. Meyer, and C. Rose, Proceedings of LINAC 2002, Gyeongju, Korea, p. 173-175, 2002.

[2] C. K. Allen, W. Blokland, S.M. Cousineau, and J.D. Galambos, Linac 2008 Conference, Victoria, British Columbia, Canada, Sept. 29 – Oct. 3, 2008.

[3] C. K. Allen, W. Blokland, S.M. Cousineau, and J.D. Galambos, HB2008 Workshop, Nashville, Tennessee, Aug. 25 – Aug. 29, 2008.

[4] H. Sako, C.K. Allen, H. Ikeda, and G. Shen, *IEEE Trans. Nucl. Science*, Vol. 57, No. 3, pp. 1528-1536 (June 2010).